ISSN 1674-1056
http://cpb.iphy.ac.cn
http://iopscience.iop.org/cpb
中国物理 B
Chinese Physics
中国物理
Chinese Physics B

Bogoliubov excitations in a Bose-Hubbard model on a hyperhoneycomb lattice

Wen-yan Zhou(周雯琰), Ya-jie Wu(吴亚杰), Su-Peng Kou(寇谡鹏)
Citation: Chin. Phys. B . 2018, 27(5): 050302. **doi:** 10.1088/1674-1056/27/5/050302

Journal homepage: http://cpb.iphy.ac.cn; http://iopscience.iop.org/cpb

What follows is a list of articles you may be interested in

Soliton excitations in a polariton condensate with defects

Abderahim Mahmoud Belounis, Salem Kessal
Chin. Phys. B . 2018, 27(1): 010307. **doi:** 10.1088/1674-1056/27/1/010307

Generating periodic interference in Bose-Einstein condensates

Shen-Tong Ji(冀慎统), Yuan-Sheng Wang(王元生), Yue-E Luo(罗月娥), Xue-Shen Liu(刘学深)
Chin. Phys. B . 2016, 25(9): 090303. **doi:** 10.1088/1674-1056/25/9/090303

Oscillation of the spin-currents of cold atoms on a ring due to light-induced spin-orbit coupling

Xie Wen-Fang, He Yan-Zhang, Bao Cheng-Guang
Chin. Phys. B . 2015, 24(6): 060305. **doi:** 10.1088/1674-1056/24/6/060305

Excitations of optomechanically driven Bose–Einstein condensates in a cavity： Photodetection measurements

Neha Aggarwal, Sonam Mahajan, Aranya B. Bhattacherjee, Man Mohan
Chin. Phys. B . 2014, 23(10): 100305. **doi:** 10.1088/1674-1056/23/10/100305

Landau damping and frequency-shift of a quadrupole mode in a disc-shaped rubidium Bose-Einstein condensate

Rahmut Arzigul, Peng Sheng-Qiang, Ma Xiao-Dong
Chin. Phys. B . 2014, 23(9): 090311. **doi:** 10.1088/1674-1056/23/9/090311

Bogoliubov excitations in a Bose–Hubbard model on a hyperhoneycomb lattice*

Wen-yan Zhou(周雯琰)[1], Ya-jie Wu(吴亚杰)[2], and Su-Peng Kou(寇谡鹏)[1,†]

[1] *Department of Physics, Beijing Normal University, Beijing* 100875, *China*
[2] *School of Science, Xi'an Technological University, Xi'an* 710032, *China*

(Received 16 November 2017; revised manuscript received 23 February 2018; published online 26 April 2018)

We study the topological properties of Bogoliubov excitation modes in a Bose–Hubbard model of three-dimensional (3D) hyperhoneycomb lattices. For the non-interacting case, there exist nodal loop excitations in the Bloch bands. As the on-site repulsive interaction increases, the system is first driven into the superfluid phase and then into the Mott-insulator phase. In both phases, the excitation bands exhibit robust nodal-loop structures and bosonic surface states. From a topology point of view, these nodal-loop excitation modes may be viewed as a permanent fingerprint left in the Bloch bands.

Keywords: hyperhoneycomb lattice, Mott-superfluid transition, Bogoliubov excitations, nodal-loop

PACS: 03.75.Kk, 67.25.dj, 37.10.Jk **DOI:** 10.1088/1674-1056/27/5/050302

1. Introduction

Owing to the existence of emergent Dirac fermions, the two-dimensional (2D) honeycomb lattice has attracted the considerable attention of researchers in condensed matter physics. Recently, the 2D honeycomb lattice was materialized in graphene, silicene and other related materials. Naturally, there is a three-dimensional (3D) extension to the honeycomb lattice, it has been addressed in a number of works in both theory and experiments, such as hyperhoneycomb[1–3] and stripyhoneycomb lattices,[3] which have been realized in β-Li_2IrO_3 and γ-Li_2IrO_3, loop-nodal semimetal[4,5] and topological insulators,[4] nodal ring,[6,7] and Weyl spinons [7] of interacting spin systems. In particular, Ezawa proposed a wide class of 3D honeycomb lattices constructed by two building blocks $[x]$ and $[y]$,[8] which subsequently facilitated the research.

According to the correspondence between bulk and edge, the energy bands of excited bosonic modes with topological structure always give rise to topologically protected edge modes. In order to understand these new exotic quantum states, there are growing efforts in searching for the topology of bosonic modes in interacting bosons on optical lattices,[9,10] photonic systems,[11,12] magnonic excitations,[13,14] phononic excitations,[15–17] polaritonic excitations,[18,19] etc. Accordingly, the topology of magnetic excitations has been widely studied recently, including magnon Chern insulators,[15,20] Weyl magnons,[21,22] magnon nodal-line semimetals[23,24] and Dirac magnons.[25] Here, we will focus on the issue of whether there are excitations with a loop structure in the 3D Bose–Hubbard extension.

In this paper, we study the properties of excitation modes in the Bose–Hubbard extension of the Hamiltonian on hyperhoneycomb lattices and offer an insight into a Bose–Einstein condensate (BEC) on the optical lattice in cold atoms. As the on-site repulsive interaction increases, the system is first driven into the superfluid (SF) phase and then into the Mott-insulator (MI) phase. We find that there exist excitations with nodal line structures on the hyperhoneycomb lattices in both SF and MI phases. Therefore, the topological properties of the excitation modes in the Bose–Hubbard model on the hyperhoneycomb lattices may be viewed as a permanent fingerprint in the Bloch bands.

The paper is organized as follows. In Section 2, we introduce the extended Bose–Hubbard model on the 3D hyperhoneycomb lattice, and then give the band structure for its non-interacting case. In Section 3, we present the phase diagram consisting of superfluid and Mott-insulator phases. In Section 4, the excitation spectra for bosonic superfluids are calculated by means of the Gross–Pitaevskii (GP) theory. In Section 5, we show the excitation spectra in the Mott-insulator phase. Finally, we conclude our discussions in Section 6.

2. Bose–Hubbard model in the hyperhoneycomb lattice

We consider bosonic atoms on a simplest 3D lattice, i.e., the hyperhoneycomb lattice. See the illustrations in Fig 1. A hyperhoneycomb lattice is a three-dimensional system. The unit cell contains two building blocks (four atoms) and each atom is connected by three coplanar bonds spaced by 120°. Each unit cell contains four atoms, of which atoms 1–3 are in

*Project supported by the National Natural Science Foundation of China (Grant Nos. 11474025, 11674026, and 11504285), Specialized Research Fund for the Doctoral Program, China, and Young Talent Fund of University Association for Science and Technology in Shaanxi, China (Grant No. 20160224).

†Corresponding author. E-mail: spkou@bnu.edu.cn

© 2018 Chinese Physical Society and IOP Publishing Ltd

the xz plane, and atoms 2–4 are in the yz plane.[5,8] The Bose–Hubbard model on the hyperhoneycomb lattice is then written as

$$H = \sum_{\langle i,j\rangle} t_{i,j} a_i^\dagger a_j - \sum_{\langle i\rangle} \mu a_i^\dagger a_i + \frac{U}{2}\sum_{\langle i\rangle} n_i(n_i-1), \quad (1)$$

where $\langle i,j\rangle$ represent the nearest neighbor sites, $t_{i,j}=t_z$ is the hopping parameter along the z-axis, and $t_{i,j}=t_{x,y}$ are other hopping parameters. In this paper, we set $t_{x,y}=t_z=-1$. a_i ($a_i^\dagger$) is the bosonic annihilation (creation) operator at the lattice site i. μ is the chemical potential, and U describes the on-site interaction between the bosons.

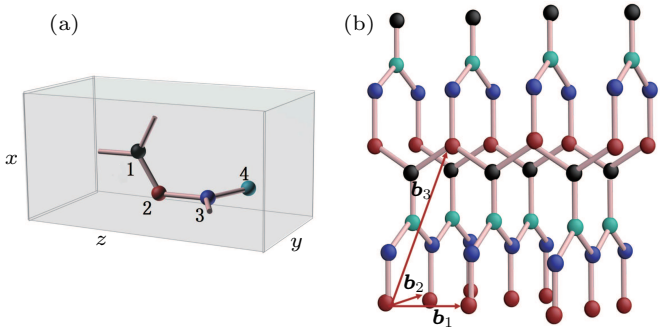


Fig. 1. (color online) (a) The building blocks of a hyperhoneycomb with four atoms per unit cell. They are located at $\boldsymbol{r}_1=(0,0,0)$, $\boldsymbol{r}_2=(-\sqrt{3}/2,0,1/2)$, $\boldsymbol{r}_3=(-\sqrt{3}/2,0,3/2)$, $\boldsymbol{r}_4=(-\sqrt{3}/2,\sqrt{3}/2,2)$ and each atom has three neighbors connected by 120° bonds. Atoms 1 and 2 form the vertical building block, atoms 3 and 4 constitute the horizontal building block. The two blocks are connected by bonds along the z-direction. (b) The simplest 3D generalization of the hyperhoneycomb lattice. The four-site unit cell and primitive translation vectors are indicated, i.e., $\boldsymbol{b}_1=(\sqrt{3}/2,0,0)$, $\boldsymbol{b}_2=(0,\sqrt{3}/2,0)$, $\boldsymbol{b}_3=(\sqrt{3}/2,\sqrt{3}/2,3)$.

We first perform a Fourier transformation on the Hamiltonian by using $a_{i\alpha}^\dagger=(\frac{1}{\sqrt{N}})\sum_k a_{k\alpha}^\dagger \mathrm{e}^{-\mathrm{i}k\cdot r_i}$, where N is the number of sites of the sublattice α, and $\alpha=1,2,3,4$ denote the four atoms in a unit cell. Then we obtain the Hamiltonian in the momentum space for the non-interacting case with $U=0$,

$$\widehat{H}_0=\sum_k \Phi_k^\dagger(h(k)-\mu)\Phi_k, \quad (2)$$

where

$$h(k)=t\begin{pmatrix} 0 & t\Theta_x & 0 & t\,\mathrm{e}^{-\mathrm{i}k_z} \\ t\Theta_x^* & 0 & t\,\mathrm{e}^{\mathrm{i}k_z} & 0 \\ 0 & t\,\mathrm{e}^{-\mathrm{i}k_z} & 0 & t\Theta_y \\ t\,\mathrm{e}^{\mathrm{i}k_z} & 0 & t\Theta_y^* & 0 \end{pmatrix}, \quad (3)$$

$\Phi_k^\dagger=(a_{1k}^*, a_{2k}^*, a_{3k}^*, a_{4k}^*)$, and $\Theta_\eta=2\,\mathrm{e}^{\mathrm{i}k_z/2}\cos(\sqrt{3}k_\eta/2)$ with $\eta=x,y$. At zero temperature, the bosons condense into the lowest energy mode at the momentum point $\boldsymbol{k}_0=(0,0,0)$. The energy line with $E=-3t$ forms a nodal loop with $k_z=0$ and $4\cos(\sqrt{3}k_x/2)\cos(\sqrt{3}k_y/2)=1$ in the momentum space. Therefore, this system exhibits nodal-loop excitations in the Bloch bands.

3. Mott–superfluid transition

As the on-site repulsive interaction increases, the system will be driven from the SF phase into MI phase. In the strong coupling limit, i.e., $U\gg t$, the bosons tend to localize to form an MI.

By the mean-field approach, which is capable of describing the Mott insulating phase, we introduce the superfluid order parameter as $\psi_{i\alpha}=\langle a_{i,\alpha}\rangle$.[26,27] Then the term $a_{i\alpha}^\dagger a_{j\alpha}$ is written as

$$a_{i\alpha}^\dagger a_{j\alpha}=a_{i\alpha}^\dagger\psi_\alpha+\psi_\alpha a_{j\alpha}-\psi_\alpha\psi_\alpha, \quad (4)$$

where j denotes the coordinate of lattice site i's nearest neighbor cell. We assume $\psi_1=\psi_{i,1}$, $\psi_2=\psi_{i,2}$, $\psi_3=\psi_{i,3}$, and $\psi_4=\psi_{i,4}$. The effective Hamiltonian is given by $H=H^0+H'$, where

$$\begin{aligned} H^0 &= \frac{U}{2}(n_1^2+n_2^2+n_3^2+n_4^2-n)-\mu n \\ &\quad -4\psi_1\psi_2-2\psi_1\psi_4-4\psi_3\psi_4-2\psi_3\psi_2, \quad (5) \\ H' &= (a_1+a_1^\dagger)(2\psi_2+\psi_4)+(a_2+a_2^\dagger)(2\psi_1+\psi_3) \\ &\quad +(a_3+a_3^\dagger)(2\psi_4+\psi_2)+(a_4+a_4^\dagger)(2\psi_3+\psi_1). \quad (6) \end{aligned}$$

In the occupation-number basis, the odd powers of the expansion of energy are always zero. Therefore, the zero-order ground state energy is given by

$$\begin{aligned} E_{\mathrm{g}}^{(0)} &= \min(e^{(0)}_{\{n_1;n_2;n_3;n_4\}}) \\ &= \frac{U}{2}(n_1^2+n_2^2+n_3^2+n_4^2-n)-\mu n \\ &\quad -4\psi_1\psi_2-2\psi_1\psi_4-4\psi_3\psi_4-2\psi_3\psi_2, \quad (7) \end{aligned}$$

where $n=n_1+n_2+n_3+n_4$, and n_1–n_4 are the particle numbers on sublattices 1–4, respectively. The second-order perturbation of energy takes the following form:

$$E_n^{(2)}=\frac{|\langle n_1;n_2;n_3;n_4|H'|k_1;k_2;k_3;k_4\rangle|^2}{E_n^{(0)}-E_k^{(0)}}, \quad (8)$$

where $k_1=n_1\pm1$, $k_2=n_2$, $k_3=n_3$, $k_4=n_4$; or $k_1=n_1$, $k_2=n_2\pm1$, $k_3=n_3$, $k_4=n_4$; or $k_1=n_1$, $k_2=n_2$, $k_3=n_3\pm1$, $k_4=n_4$; or $k_1=n_1$, $k_2=n_2$, $k_3=n_3$, $k_4=n_4\pm1$. We readily obtain the ground-state energy in terms of the order parameter ψ

$$\begin{aligned} E &\approx a_0+a_{21}\psi_1^2+a_{22}\psi_2^2+b_{21}\psi_3^2+b_{22}\psi_4^2 \\ &\quad +c_1\psi_1\psi_2+c_2\psi_1\psi_3+c_3\psi_1\psi_4+c_4\psi_2\psi_3 \\ &\quad +c_5\psi_2\psi_4+c_6\psi_3\psi_4+O(\psi_1^4,\psi_2^4,\psi_3^4,\psi_4^4), \quad (9) \end{aligned}$$

where coefficients a_0, a_{21}, a_{22}, b_{21}, b_{22}, c_1, c_2, c_3, c_4, c_5, and c_6 are

$$\begin{aligned} a_0 &= (n_1^2+n_2^2+n_3^2+n_4^2-n)U/2-\mu n, \quad (10) \\ a_{21} &= \frac{4(-U-\mu)}{[(n_2-1)U-\mu][-n_2U+\mu]} \\ &\quad +\frac{(-U-\mu)}{[(n_4-1)U-\mu][-n_4U+\mu]}, \quad (11) \end{aligned}$$

$$a_{22} = \frac{4(-U-\mu)}{[(n_1-1)U-\mu][-n_1U+\mu]} + \frac{(-U-\mu)}{[(n_3-1)U-\mu][-n_3U+\mu]}, \quad (12)$$

$$b_{21} = \frac{4(-U-\mu)}{[(n_4-1)U-\mu][-n_4(U+\mu)]} + \frac{(-U-\mu)}{[(n_2-1)U-\mu][-n_2U+\mu]}, \quad (13)$$

$$b_{22} = \frac{(-U-\mu)}{[(n_1-1)U-\mu][-n_1U+\mu]} + \frac{4(-U-\mu)}{[(n_3-1)U-\mu][-n_3U+\mu]}, \quad (14)$$

$$c_1 = c_6 = -4, \quad (15)$$

$$c_2 = \frac{4(-U-\mu)}{[(n_2-1)U-\mu][-n_2U+\mu]} + \frac{4(-U-\mu)}{[(n_4-1)U-\mu][-n_4U+\mu]}, \quad (16)$$

$$c_3 = c_4 = -2, \quad (17)$$

$$c_5 = \frac{4(-U-\mu)}{[(n_3-1)U-\mu][-n_3U+\mu]} + \frac{4(-U-\mu)}{[(n_1-1)U-\mu][-n_1U+\mu]}. \quad (18)$$

By means of the usual Landau procedure for second-order phase transitions, the points corresponding to the secondary derivative coefficients to superfluid order being zero form the phase boundary between the superfluid phase and the MI phase. Therefore, to derive the solutions of phase transition, we should consider the second-order derivation[28] to determinate $D(E)$, where $D \equiv \det(D)$, $D_{i,j} = \partial\psi_i\partial\psi_j$, $i,j = 1,2,3,4$. At the point $E_0 = E(\psi_1 = 0,\ \psi_2 = 0,\ \psi_3 = 0,\ \psi_4 = 0)$, the derivative is obtained as

$$\det\begin{bmatrix} 2a_{21} & c_1 & c_2 & c3 \\ c_1 & 2a_{22} & c_4 & c_5 \\ c_2 & c_4 & 2b_{21} & c_6 \\ c_3 & c_5 & c_6 & 2b_{22} \end{bmatrix}. \quad (19)$$

For the case of $D(E_0) = 0$, the insulating phase is no longer stable and a phase transition occurs. One can obtain the function of phase-transition line (we chose $\widetilde{n} = n_1 = n_2 = n_3 = n_4$)

$$\mu = \frac{1}{2}(-3 + (2\widetilde{n}-1)U \pm \sqrt{9 - 6(2\widetilde{n}+1)U + U^2}), \quad (20)$$

where the subscripts $\pm$ denote the two halves of the Mott insulating regions in phase space. Figure 2 shows a plot of Eq. (21) for $\widetilde{n} = 1,2,3$. Correspondingly, we can find the critical point of the smallest on-site interaction

$$U_c = 3(1 + 2\widetilde{n} + 2\sqrt{\widetilde{n} + \widetilde{n}^2}). \quad (21)$$

By applying the Landau theory and the second-order perturbation theory of phase transitions, we obtain the phase diagram shown in Fig. 2. It shows that the phase transition occurs at $U_c = U/t \approx 17.485$ for the MI(1,1,1,1) lobe with the particle number configuration $\{n_1 = 1,\ n_2 = 1,\ n_3 = 1,\ n_4 = 1\}$.

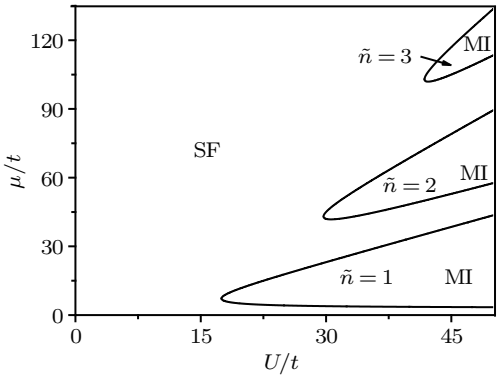


Fig. 2. The phase diagram of the Bose–Hubbard model on a 3D hyperhoneycomb lattice by the second-order perturbation theory. The vertical and horizontal axes represent the dimensionless parameters of the chemical μ/t and the interaction strength U/t.

4. Excitation modes for the superfluid

The excitation spectra are related to the collective modes of the BEC. In this section, by means of the Gross–Pitaevskii (GP) theory, we discuss excitations from the condensate ground state of the Bose–Hubbard model on the hyperhoneycomb lattice.

For weak interaction strength $U < U_c$, the system will be in the superfluid phase. We use the following mean-field approximation:[29]

$$\langle a_{r_i\alpha}\rangle = \psi_{r_i\alpha}. \quad (22)$$

By replacing $(a^\dagger_{r_i\alpha}, a_{r_i\alpha})$ by $(\psi^\dagger_{r_i\alpha}, \psi_{r_i\alpha})$ in the Hamiltonian in Eq. (1), the following energy function is obtained

$$\begin{aligned} H &= \sum_{\langle i,j\rangle} t_{i,j}a^\dagger_i a_j - \sum_{\langle i\rangle}\mu a^\dagger_i a_i + \frac{U}{2}\sum_{\langle i\rangle} n_i(n_i-1) \\ &= t\sum_{R_i,R_j} \psi^\dagger_{1r_i}\psi_{2r_i} + \psi^\dagger_{1r_i}\psi_{2r_j} + \psi^\dagger_{1r_i}\psi_{4r_j} \\ &\quad + \psi^\dagger_{2r_i}\psi_{1r_i} + \psi^\dagger_{2r_j}\psi_{1r_i} + \psi^\dagger_{2r_i}\psi_{3r_i} \\ &\quad + \psi^\dagger_{3r_i}\psi_{2r_i} + \psi^\dagger_{3r_i}\psi_{4r_i} + \psi^\dagger_{3r_j}\psi_{4r_i} \\ &\quad + \psi^\dagger_{4r_i}\psi_{3r_i} + \psi^\dagger_{4r_i}\psi_{3r_j} + \psi^\dagger_{4r_j}\psi_{1r_i} \\ &\quad + \frac{U}{2}\sum_{\langle j\rangle}[\psi^\dagger_{1r_j}\psi_{1r_j}(\psi^\dagger_{1r_j}\psi_{1r_j} - 1)]. \end{aligned} \quad (23)$$

Here, we consider the homogeneous case that refers to the situation where the system has the periodicity of the lattice. The ground state wave function of the BEC can be well described by the GP equation

$$\mathrm{i}\frac{\partial\psi}{\partial t} = \frac{\delta E}{\delta\psi^*}. \quad (24)$$

So we can obtain the equations

$$\mathrm{i}\frac{\partial\psi_1}{\partial t} = t(\psi_2 + \psi_{2'} + \psi_4) + \frac{U}{2}(2|\psi_1|^2\psi_1 - \psi_1) - \mu\psi_1,$$

$$
\begin{aligned}
\mathrm{i}\frac{\partial\psi_2}{\partial t} &= t(\psi_1+\psi_{1'}+\psi_3)\\
&\quad+\frac{U}{2}(2|\psi_2|^2\psi_2-\psi_2)-\mu\psi_2,\\
\mathrm{i}\frac{\partial\psi_3}{\partial t} &= t(\psi_4+\psi_{4'}+\psi_2)\\
&\quad+\frac{U}{2}(2|\psi_3|^2\psi_3-\psi_3)-\mu\psi_3,\\
\mathrm{i}\frac{\partial\psi_4}{\partial t} &= t(\psi_3+\psi_{3'}+\psi_1)\\
&\quad+\frac{U}{2}(2|\psi_2|^2\psi_4-\psi_4)-\mu\psi_4. \qquad (25)
\end{aligned}
$$

After considering the quantum fluctuations of the condensate, the order parameters become[30]

$$
\begin{aligned}
\psi_1 &= \sqrt{n}+A\,\mathrm{e}^{\mathrm{i}(kr_i-\omega t)}+B^*\,\mathrm{e}^{-\mathrm{i}(kr_i-\omega t)},\\
\psi_2 &= \sqrt{n}+C\,\mathrm{e}^{\mathrm{i}(kr_i-\omega t)}+D^*\,\mathrm{e}^{-\mathrm{i}(kr_i-\omega t)},\\
\psi_3 &= \sqrt{n}+E\,\mathrm{e}^{\mathrm{i}(kr_i-\omega t)}+F^*\,\mathrm{e}^{-\mathrm{i}(kr_i-\omega t)},\\
\psi_4 &= \sqrt{n}+G\,\mathrm{e}^{\mathrm{i}(kr_i-\omega t)}+H^*\,\mathrm{e}^{-\mathrm{i}(kr_i-\omega t)}, \qquad (26)
\end{aligned}
$$

where A, B, C, D, E, F, G, H are small complex parameters, r_i is the position of the lattice site, and k is the reciprocal lattice vector. After plugging these wave functions into the GP function, and keeping the linear terms of A, B, C, D, E, F, G, H, we obtain

$$
\begin{aligned}
\omega A &= 2t\cos\left(\frac{\sqrt{3}}{2}k_x\right)\mathrm{e}^{\mathrm{i}\frac{k_z}{2}}C+tG\,\mathrm{e}^{-\mathrm{i}k_z}\\
&\quad+2UnA+UnB-\left(\frac{Un}{2}+\mu\right)A, \qquad (27)\\
\omega B &= -2t\cos\left(\frac{\sqrt{3}}{2}k_x\right)\mathrm{e}^{\mathrm{i}\frac{k_z}{2}}D-tH\,\mathrm{e}^{-\mathrm{i}k_z}\\
&\quad-2UnB-UnA+\left(\frac{Un}{2}+\mu\right)B, \qquad (28)
\end{aligned}
$$

$$
\begin{aligned}
\omega C &= 2t\cos\left(\frac{\sqrt{3}}{2}k_x\right)\mathrm{e}^{-\mathrm{i}\frac{k_z}{2}}A+tE\,\mathrm{e}^{\mathrm{i}k_z}\\
&\quad+2UnC+UnD-\left(\frac{Un}{2}+\mu\right)C, \qquad (29)\\
\omega D &= -2t\cos\left(\frac{\sqrt{3}}{2}k_x\right)\mathrm{e}^{-\mathrm{i}\frac{k_z}{2}}B-tF\,\mathrm{e}^{\mathrm{i}k_z}\\
&\quad-2UnD-UnC+\left(\frac{Un}{2}+\mu\right)D, \qquad (30)\\
\omega E &= 2t\cos\left(\frac{\sqrt{3}}{2}k_y\right)\mathrm{e}^{\mathrm{i}\frac{k_z}{2}}G+tC\,\mathrm{e}^{-\mathrm{i}k_z}\\
&\quad+2nE+UnF-\left(\frac{Un}{2}+\mu\right)E, \qquad (31)\\
\omega F &= -2t\cos\left(\frac{\sqrt{3}}{2}k_y\right)\mathrm{e}^{\mathrm{i}\frac{k_z}{2}}H-tD\mathrm{e}^{-\mathrm{i}k_z}\\
&\quad-2UnF-UnE+\left(\frac{Un}{2}+\mu\right)F, \qquad (32)\\
\omega G &= 2t\cos\left(\frac{\sqrt{3}}{2}k_y\right)\mathrm{e}^{-\mathrm{i}\frac{k_z}{2}}E+tA\,\mathrm{e}^{\mathrm{i}k_z}\\
&\quad+2UnG+UnH-\left(\frac{Un}{2}+\mu\right)G, \qquad (33)\\
\omega H &= -2t\cos\left(\frac{\sqrt{3}}{2}k_y\right)\mathrm{e}^{-\mathrm{i}\frac{k_z}{2}}F-tB\mathrm{e}^{\mathrm{i}k_z}\\
&\quad-2UnH-UnG+\left(\frac{Un}{2}+\mu\right)H. \qquad (34)
\end{aligned}
$$

The chemical potential is $\mu=3t+Un-Un/2$. Next, we simplify Eqs. (27)–(34) to an algebraic equation of the form

$$H_{\mathrm{gp}}\Psi=\omega\Psi, \qquad (35)$$

where

$$\Psi=(A,\ B,\ C,\ D,\ E,\ F,\ G,\ H), \qquad (36)$$

$$
H_{\mathrm{gp}}=\begin{pmatrix}
E_0 & Un & t\Theta_x & 0 & 0 & 0 & t\,\mathrm{e}^{-\mathrm{i}k_z} & 0\\
-Un & -E_0 & 0 & -t\Theta_x & 0 & 0 & 0 & -t\,\mathrm{e}^{-\mathrm{i}k_z}\\
t\Theta_x^* & 0 & E_0 & Un & t\,\mathrm{e}^{\mathrm{i}k_z} & 0 & 0 & 0\\
0 & -t\Theta_x^* & -Un & -E_0 & 0 & -t\,\mathrm{e}^{\mathrm{i}k_z} & 0 & 0\\
0 & 0 & t\,\mathrm{e}^{-\mathrm{i}k_z} & 0 & E_0 & Un & t\Theta_y & 0\\
0 & 0 & 0 & -t\,\mathrm{e}^{-\mathrm{i}k_z} & -Un & -E_0 & 0 & -t\Theta_y\\
t\,\mathrm{e}^{\mathrm{i}k_z} & 0 & 0 & 0 & t\Theta_y^* & 0 & E_0 & Un\\
0 & -t\,\mathrm{e}^{\mathrm{i}k_z} & 0 & 0 & 0 & -t\Theta_y^* & -Un & -E_0
\end{pmatrix}, \qquad (37)
$$

with $\Theta_\eta=2\cos(\frac{\sqrt{3}}{2}k_\eta)\,\mathrm{e}^{\mathrm{i}\frac{k_z}{2}}$, $\eta=x,y$, and $E_0=-3t+Un$. The energy spectrum can be obtained by calculating the eigenvalues of H. The results are shown in Fig. 3. From the figure, one can see that there is a nodal loop in the excitation bands when $E=E_0$. The results indicate that the loop structure has no significant change as the interaction strength increases in the SF phase.

In order to study the topological properties of the excitation modes of quasiparticles, we calculate the Berry phases[31,32] for paths in momentum space that encircle the nodal line[33]

$$P_{\mathrm{B}}=-\oint\mathrm{i}\left\langle\Phi_k^{(2)}\middle|\nabla_k\Phi_k^{(2)}\right\rangle\mathrm{d}\boldsymbol{k}, \qquad (38)$$

where $\Phi_k^{(2)}$ is the wave-function. We divide the path into N_j intervals with $\alpha_j=2(j-1)\pi/N_j$ as[34]

$$P_{\mathrm{B}} = -\int_0^{2\pi} \mathrm{i}\left\langle \Phi_\alpha^{(2)} \middle| \nabla_\alpha \Phi_\alpha^{(2)} \right\rangle \mathrm{d}\alpha \approx \sum_{j=1}^{N_j} \mathrm{Arg}\left[\left\langle \Phi_{\alpha_j}^{(2)} \middle| \Phi_{\alpha_{j+1}}^{(2)} \right\rangle\right]. \quad (39)$$

After direct numerical calculations, for a closed loop encircling the nodal lines, we find the Berry phase $P_{\mathrm{B}} = \pi$, which indicates that the flat surface states exist.[35]

In addition, we apply the GP theory to study the edge modes of SF on the hyperhoneycomb lattice, where the system is finite along the z direction and the momentum k_x and k_y remain good quantum numbers. For certainty, we show the band structures of surface excitations on the zigzag edge of the SF in Fig. 4. It shows that there are partial flat bands appearing in the outer region of the loop structure when both edges are terminated by the zigzag edge, which is similar to the case of the fermionic system.[8]

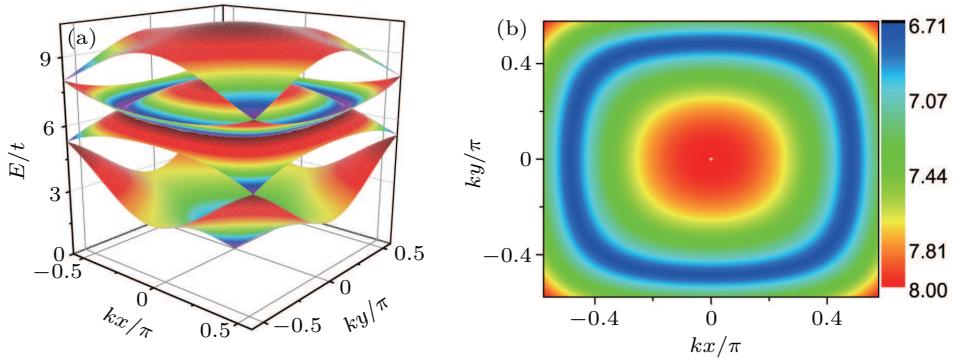


Fig. 3. (color online) (a) The energy spectra of excitations with fixed $k_z = 0$ and $Un/t = 5$. (b) The contour plot of the energy spectra of the third band from the bottom up of the quasiparticle-excitation modes with fixed $k_z = 0$ and $Un/t = 5$, the nodal loop structure is presented by the blue loop.

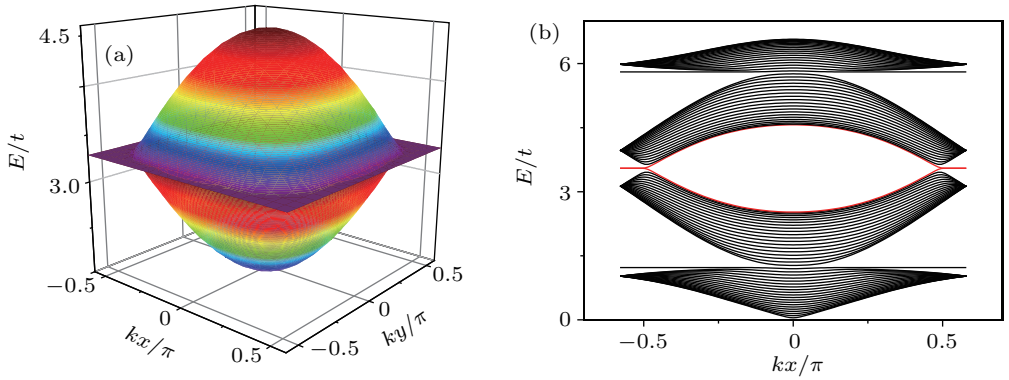


Fig. 4. (color online) (a) Band structures of a slab with finite width along the z-direction. Here we set $Un/t = 0.6$. In particular, the edge states are partial flat bands. (b) Band structures of a slab with finite width along the z-direction and $k_y = 0$. Here we set $Un/t = 0.6$. The edge states are indicated by the red lines.

5. Excitation modes for the MI phase

In this section, we calculate the quasiparticle and quasihole dispersions using a functional integral formalism.[26] We first define complex functions $a_i(\tau)$ and $a_i^*(\tau)$. The partition function of the system is written as a function integral

$$Z = \mathrm{Tr}\,\mathrm{e}^{-\beta\widehat{H}} = \int \mathcal{D}a^*\mathcal{D}a \exp\{-S[a^*,a]/\hbar\}, \quad (40)$$

with $\beta = \frac{1}{k_{\mathrm{B}}T}$, where k_{B} is the Boltzman constant. The action $S[a^*,a]$ is given by

$$S[a^*,a] = \int_0^{\hbar\beta} \mathrm{d}\tau \left[\sum_i a_i^*(\tau)\left(\hbar\frac{\partial}{\partial\tau} - \mu\right)a_i(\tau) + H_0(\tau) + \frac{1}{2}U\sum_i a_i^*(\tau)a_i^*(\tau)a_i(\tau)a_i(\tau)\right].$$

To decouple the hopping terms, we rewrite the action by using the Hubbard–Stratonovich transformation as in Ref. [26]. Then the effective action is explicitly expressed as

$$S[a^*,a,\psi^*,\psi] = \int_0^{\hbar\beta} \mathrm{d}\tau \left[\sum_i a_i^*\left(\hbar\frac{\partial}{\partial\tau} - \mu\right)a_i + \frac{1}{2}U\sum_i a_i^* a_i^* a_i a_i - \sum_{ij} t_{ij}(a_i^*\psi_j + \psi_i^* a_j) + \sum_{ij} t_{ij}\psi_i^*\psi_j\right], \quad (41)$$

where ψ^* and ψ are the order parameter fields. After integrating out the complex fields $a_i(\tau)$ and $a_i^*(\tau)$, we can obtain the effective action up to the second order as

$$S^{\mathrm{eff}}[\psi^*,\psi] \approx S^{(0)} + S^{(2)}, \quad (42)$$

with

$$S^{(2)}[\psi^*,\psi]$$

$$= \int_0^{\hbar\beta} \mathrm{d}\tau \sum_{ij} \psi_i^* t_{ij} \psi_j - \frac{1}{\hbar} \int_0^{\hbar\beta}\int_0^{\hbar\beta} \mathrm{d}\tau \mathrm{d}\tau' \sum_{iji'j'} t_{ij} t_{i'j'} \times \psi_j^*(\tau) \left\langle T_\tau \left[b_i(\tau) b_{i'}^*(\tau') \right] \right\rangle_{S^{(0)}} \psi_{j'}(\tau'). \quad (43)$$

The zero-order action $S^{(0)}$ goes to zero near the phase transformation point. So we can readily obtain the effective action near the phase transformation point in momentum space by the Fourier transformation

$$S^{\mathrm{eff}}[\psi^*, \psi] = \sum_{k,m} \left(\Phi_k^*(\tau)(\mathcal{H} - \mathcal{H}^2 f_{\omega_m}) \Phi_k(\tau) \right) = \sum_{k,m} (\Phi_k^*(\tau)(-\mathcal{G}^{-1}(k, \mathrm{i}\omega_m)) \Phi_k(\tau)), \quad (44)$$

with

$$H = \begin{pmatrix} 0 & c_1 & 0 & d_1 \\ c_2 & 0 & d_2 & 0 \\ 0 & d_1 & 0 & w_1 \\ d_2 & 0 & w_2 & 0 \end{pmatrix}, \quad (45)$$

where $\Phi_k(\tau) = (\phi_{k_1}(\tau), \phi_{k_2}(\tau), \phi_{k_3}(\tau), \phi_{k_4}(\tau))$, $c_1 = c_2^* = 2t\,\mathrm{e}^{\mathrm{i}k_z/2} \cos(\sqrt{3}k_x/2)$, $w_1 = w_2^* = 2t\,\mathrm{e}^{\mathrm{i}k_z/2} \cos(\sqrt{3}k_y/2)$, and $d_1 = d_2^* = t\,\mathrm{e}^{-\mathrm{i}k_z}$.

By substituting $\mathrm{i}\omega_m \to \omega_m$, we can obtain a function of real energies $\hbar\omega$

$$\det\left[G^{-1}\right] = 0. \quad (46)$$

The quasiparticle and quasihole dispersions are given by

$$\hbar\omega_{i,\mathrm{qp,ph}} = \frac{1}{2}\left[-2\mu + (2n-1)U - \frac{1}{f_{\omega_{m_i}}} \pm \Delta E_{i,k} \right], \quad (47)$$

with

$$\Delta E_{i,k} = \sqrt{U^2 - \frac{(4n+2)U}{f_{\omega_{m_i}}} + \frac{1}{f_{\omega_{m_i}}^2}}, \quad (48)$$

$$f_{\omega_{m_i}} = \pm\sqrt{\frac{c_1 c_2 + 2d_1 d_2 + w_1 w_2}{2A} \pm \frac{\sqrt{B}}{2A}}, \quad (49)$$

where

$$A = d_1^2 d_2^2 - c_1 d_2^2 w_1 - c_2 d_1^2 w_2 + c_1 c_2 w_1 w_2, \quad (50)$$

$$B = c_1^2 c_2^2 + 4c_1 c_2 d_1 d_2 + 4c_1 d_2^2 w_1 + 4c_2 d_1^2 w_2 - 2c_1 c_2 w_1 w_2 + 4d_1 d_2 w_1 w_2 + w_1^2 w_2^2. \quad (51)$$

We present the energy spectra of excitation modes in the MI phase in Fig. 5. It shows that there also exists a nodal-loop structure in the excitation spectra in the MI phase, and the Mott gap becomes large as the interaction strength increases, which is similar to the case in conventional Bose–Hubbard models.

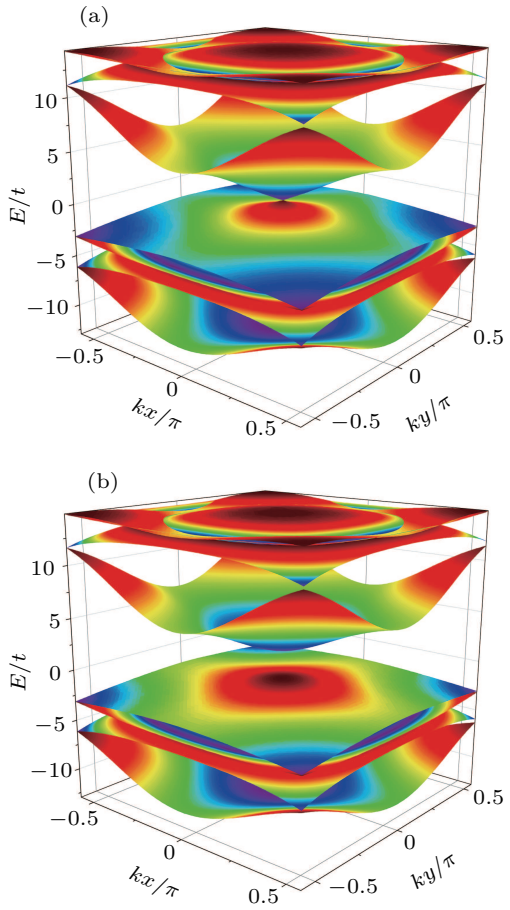


Fig. 5. (color online) (a) The energy spectra of quasiparticle and quasihole excitations with fixed $k_z = 0$ and $Un/t = 17.485$ at the MI–SF transition point. (b) The energy spectra of quasiparticle and quasihole excitations with fixed $k_z = 0$ and $Un/t = 18.0$ in the MI(1,1,1,1) phase.

6. Discussion and conclusion

In this paper, starting from the Bose–Hubbard extension of the Hamiltonian on hyperhoneycomb lattices, we study the properties of the excitation modes. In particular, we find that there exist excitations with nodal loop structures on hyperhoneycomb lattices in both SF and MI phases. Therefore, the topological properties of the excitation modes in the Bose–Hubbard model on hyperhoneycomb lattices may be viewed as a permanent fingerprint in the Bloch bands.

Finally, we discuss its possible realization in cold atoms. The Hamiltonian of the hyperhoneycomb lattice in Eq. (2) on 3D optical lattices has been proposed by using laser-assisted tunneling in Ref. [36]. By using the Feshbach resonance technique, the interaction between the particles can be tuned readily. As a result, this work may provide us with a possible scheme to realize Bogoliubov excitations with nodal loop structures in a bosonic system.

References

[1] Takayama T, Kato A, Dinnebier R, Nuss J, Kono H, Veiga L S I, Fabbris G, Haskel D and Takagi H 2015 *Phys. Rev. Lett.* **114** 077202
[2] Biffin A, Johnson R D, Choi S, Freund F, Manni S, Bombardi A, Manuel P, Gegenwart P and Coldea R 2014 *Phys. Rev. B* **90** 205116

[3] Modic K A, Smidt T E, Kimchi I, Breznay N P, Biffin A, Choi S, Johnson R D, Coldea R, Watkins-Curry P, McCandless G T, Gandara F, Islam Z, Vishwanath A, Chan J Y, Shekhter A, McDonald R D and Analytis J G 2014 *Nat. Commun.* **5** 4203

[4] Lee E K, Bhattacharjee S, Hwang K, Kim H, Jin H and Kim Y 2014 *Phys. Rev. B* **89** 205132

[5] Mullen K, Uchoa B and Glatzhofer D T 2015 *Phys. Rev. Lett.* **115** 026403

[6] Hermanns M, O'Brien K and Trebst S 2015 *Phys. Rev. Lett.* **114** 157202

[7] Schaffer R, Lee E K, Lu Y M and Kim Y B 2015 *Phys. Rev. Lett.* **114** 116803

[8] Ezawa M 2016 *Phys. Rev. Lett.* **116** 127202

[9] Furukawa S and Ueda M 2015 *New J. Phys.* **17** 115014

[10] Wu Y J, Zhou W Y and Kou S P 2017 *Phys. Rev. A* **95** 023620

[11] Peano V, Houde M, Brendel C, Marquardt F and Clerk A A 2016 *Nat. Commun.* **7** 10779

[12] Peano V, Houde M, Marquardt F and Clerk A A 2016 *Phys. Rev. X* **6** 041026

[13] Prodan E and Prodan C 2009 *Phys. Rev. Lett.* **103** 248101

[14] Süsstrunk R and Huber S D 2015 *Science* **349** 6243

[15] Shindou R, Matsumoto R, Murakami S and Ohe J 2013 *Phys. Rev. B* **87** 174427

[16] Shindou R, Ohe J, Matsumoto R, Murakami S and Saitoh E 2013 *Phys. Rev. B* **87** 174402

[17] Li Y, Zhong W X, Wang D Q, Feng Q R, Liu Z X, Zhou J F, Jia C Y, Hu F, Zeng J W, Guo Q C, Fu L and Luo M M 2016 *Nat. Commun.* **7** 10503

[18] Bardyn C E, Karzig T, Refael G and Liew T C 2015 *Phys. Rev. B* **91** 161413

[19] Karzig T, Bardyn C E, Lindner N H and Refael G 2015 *Phys. Rev. X* **5** 031001

[20] Zhang L F, Ren J, Wang J S and Li B W 2013 *Phys. Rev. B* **87** 144101

[21] Zhang C L, Xu S Y, Belopolski I, Yuan Z J, Lin Z Q, Tong B B, Alidoust N, Lee C C, Huang S M and Lin H 2016 *Nat. Commun.* **7** 10735

[22] Kim S K, Ochoa H, Zarzuela R and Tserkovnyak Y 2016 *Phys. Rev. Lett.* **117** 227201

[23] Mook A, Henk J and Mertig I 2017 *Phys. Rev. B* **95** 014418

[24] Li K K, Li C Y, Hu J P and Fang C 2017 *Phys. Rev. Lett.* **119** 247202

[25] Li K K, Li C Y, Hu J P, Li Y and Fang C 2017 *Chin. Phys. Lett.* **34** 077501)

[26] Oosten D V, Straten P V D and Stoof H T C 2001 *Phys. Rev. A* **63** 053601

[27] Lim L K, Smith C M and Hemmerich A 2008 *PPhys. Rev. Lett.* **100** 130402

[28] Chen B L, Kou S P, Zhang Y and Chen S 2010 *Phys. Rev. A* **81** 053608

[29] Keleş, Ahmet and Oktel and Oktel M Ö 2015 *Phys. Rev. A* **91** 013629

[30] Landau L D and Lifshitz E M 1980 *Course of Theoretical Physics* **5**

[31] Heikkilä T T and Volovik G E 2011 *Jetp Lett.* **93** 59

[32] Xiao D, Chang M C and Niu Q 2010 *Rev. Mod. Phys.* **82** 1959

[33] Yu R, Weng H M, Fang Z, Dai X and Hu X 2015 *Phys. Rev. Lett.* **115** 036807

[34] Fukui T, Hatsugai Y and Suzuki H 2005 *J. Phys. Soc. Jpn.* **74** 1674

[35] Huang B B and Yang X S 2018 *J. Phys. B: At. Mol. Opt. Phys.* **51** 015302

[36] Mullen K, Uchoa B, Wang B and Glatzhofer D 2017 arXiv:1603.01647